

Optical Pumping of Poly(3-hexylthiophene) Singlet Excitons Induces Charge Carrier Generation

Patrick C. Tapping and Tak W. Kee*

Department of Chemistry, The University of Adelaide, South Australia 5005, Australia

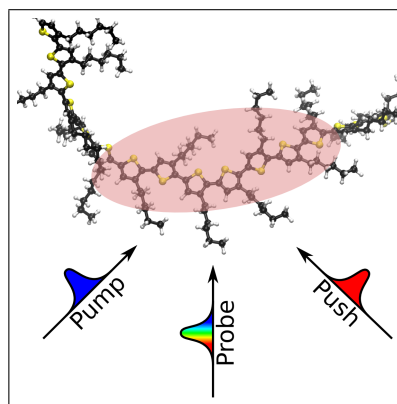
E-mail: tak.kee@adelaide.edu.au

Phone: +61-8-8313-5039

Abstract

The dynamics of high-energy excitons of poly(3-hexylthiophene) (P3HT) are shown to consist of torsional relaxation and exciton dissociation to form free carriers. In this work we use pump-push-probe femtosecond transient absorption spectroscopy to study the highly excited states of P3HT in solution. P3HT excitons are generated using a pump pulse (400 nm) and allowed to relax to the lowest-lying excited state before re-excitation using a push pulse (900 nm or 1200 nm), producing high-energy excitons which decay back to the original excited state with both sub-picosecond (0.16 ps) and picosecond (2.4 ps) time constants. These dynamics are consistent with P3HT torsional relaxation, with the 0.16-ps time constant assigned to ultrafast inertial torsional relaxation. Additionally, the signal exhibits an incomplete recovery, indicating dissociation of high-energy excitons to form charge carriers due to excitation by the push pulse. Our analysis indicates that charge carriers are formed with a yield of 11%.

Graphical TOC Entry



Keywords

P3HT, pump-push-probe spectroscopy, transient absorption, torsional relaxation, polaron

The intense research on conjugated polymers is mainly driven by the function of these materials as light harvesting chromophores and electron donors in organic solar cells.¹⁻⁴ Polymer based solar cells offer the advantage of solution processability for rapid and low-cost fabrication of mechanically flexible devices. Poly(3-hexylthiophene) (P3HT) is one of the most studied conjugated polymers for several important reasons. First, there are well-established synthetic methods by which a high regioselectivity is achieved routinely.⁵ Second, P3HT exhibits the ability to aggregate in an ordered fashion to form semicrystalline domains.⁶ Recent work has shown that these semicrystalline domains enhance exciton and charge transport.⁷ In many cases, long-range order is maintained and P3HT is able to “crystallize” to form nanofibers which are microns in length.⁸⁻¹⁰ In addition to nanofibers, P3HT is capable of folding into roughly spherical aggregates, *i.e.*, nanoparticles, to give rise to functional properties including charge storage and chemical sensing.^{11,12} Furthermore, P3HT nanoparticles provide a good model system for investigating the dynamics of excitons and polarons.¹³ The nanoparticle system offers a device-like environment without the significant structural and interfacial heterogeneities found in a thin-film device, thereby improving the understanding between a material’s function and its molecular properties.¹² Finally, the P3HT-fullerene blend is the most widely investigated donor-acceptor system owing to its relatively high solar power conversion efficiency, which is as high as 6.5%.¹⁴⁻¹⁶ As a consequence, there is continuing effort in studying P3HT to develop insight into the photovoltaic properties of P3HT-fullerene solar cells.

The use of femtosecond laser spectroscopy has offered a vast level of information about exciton dynamics of P3HT films or aggregates.^{13,17-24} The photoexcitation event first generates a “hot” singlet exciton with Frenkel-exciton characteristics and a spatial extent of nearly 9 nm, over approximately 20 monomeric units.²⁰ This delocalized exciton then undergoes rapid self-localization within the first 100 fs to a size of ≤ 10 monomers.¹⁹ Furthermore, vi-

brational relaxation, torsional relaxation and exciton hopping occur on the subpicosecond to >10 -picosecond time scales to enable the exciton to relax further.^{19,25} The exciton self-localization and relaxation processes produce a significant Stokes shift in the emission spectrum and exhibit a large decrease in the polarization anisotropy.¹⁹ In the case of the P3HT-fullerene films or aggregates, there is increasing evidence to suggest that charge carriers are generated at $t \leq 100$ fs.^{20,26} The large spatial extent of the initially prepared delocalized exciton offers the opportunity for a significant fraction of the “hot” exciton to be quenched by fullerene to generate free carriers. This phenomenon has also been reported for other conjugated polymer-fullerene blends recently.²⁷⁻²⁹

To obtain further insight into the behavior of excitons and charge carriers, more elaborate experimental configurations utilizing three or more optical pulses were employed. Recently, Busby et al. used pump-dump-probe spectroscopy to investigate excited-state self-trapping and ground-state relaxation dynamics of P3HT.³⁰ Wells and Blank employed two-color three-pulse photon echo peak shift spectroscopy to demonstrate that the early-time exciton relaxation of P3HT is strongly driven by the coupling between the exciton and the torsional degrees of freedom.²⁵ Other examples of multi-pulse spectroscopic investigations include coherent intrachain energy migration using 2D electronic spectroscopy, and charge carrier generation and torsional relaxation using pump-push-probe spectroscopy.³¹⁻³⁴ Notably, Gadermaier et al. used pump-push-probe spectroscopy to investigate methyl-substituted ladder-type poly(para)phenyl.³⁴ In their study, the pump pulse excites the conjugated polymer to generate singlet excitons. The push pulse then arrives at $t < 3$ ps to excite these “hot” excitons. Using this experimental scheme, the authors reported that charge carriers are generated by “pushing” the singlet excitons with a yield of 7%.

In this study, we employ pump-push-probe spectroscopy to study the effect of photoexcitation of singlet excitons of P3HT on torsional relaxation and charge carrier genera-

tion dynamics. P3HT is investigated at a low concentration under the single-chains condition to exclude contributions from interchain coupling.^{22,25,30} In the experiment, the pump pulse, with a wavelength of 400 nm, generates singlet excitons. The push pulse, which is tuned to the singlet exciton absorption band, arrives approximately 25 ps after the pump pulse to promote the relaxed or “cool” singlet excitons to high-energy, delocalized excitonic states. The probe pulse, which is centered either at the singlet exciton absorption band or the stimulated emission (SE) band, detects the effects of the pump and push pulses. The results show that most of the high-energy excitons undergo rapid relaxation back to the lowest-lying singlet excitonic state due to ultrafast torsional motions of P3HT. Approximately 11% of the high-energy excitons dissociate to form charge carriers, which in turn undergo geminate recombination to produce ground-state P3HT. The results also indicate that the exciton binding energy is ≤ 1 eV. In short, pump-push-probe spectroscopy is used to reveal new insight into the exciton dynamics of P3HT

Figure 1a shows that P3HT in tetrahydrofuran (THF) has a ground-state absorption band centered around 450 nm and it exhibits a large Stokes shift, with an emission maximum around 575 nm. Upon excitation, a broad excited-state absorption (ESA) band centered around 1100 nm appears in the near-IR region. It shows a lifetime of approximately 500 to 600 ps and has previously been assigned to the singlet exciton.^{13,35,36} Fluorescence lifetime results confirm a singlet exciton lifetime of 530 ps, which is in agreement with previously obtained values for P3HT in solution.^{19,22,23} Consequently, the pump-probe and pump-push-probe transient absorption data were fitted with a fixed time constant of 530 ps, as is discussed below. The emission signal shows a dynamic red-shift from 0 ps to ~ 25 ps.^{19,22,23} Similarly, a red-shift is also evident in the stimulated emission band of the pump-probe data, with the peak shifting from 575 to 625 nm over a period of approximately 25 ps. These results are shown in Supporting Information. This dynamic red-shift has been observed previously in polythiophene

solutions and attributed to a combination of exciton hopping and torsional relaxation.³⁷ These photophysical processes are shown in Figure 1b. Torsional motions between thiophene rings act to increase the planarization of the polymer, thereby increasing conjugation length and allowing a reduction in the energy of the exciton prior to emission.^{22,30} Similarly, the exciton is able to hop from the site of the initial excitation to lower energy chromophores in the polymer chain through excitonic energy transfer (EET), with corresponding dissipation of energy by further torsional and vibrational relaxation.³⁸

Figure 2a shows the change in optical density (ΔOD) at 1050 nm as a function of pump-probe time delay (blue circles). The photophysical processes involved in the pump-probe experiment are shown in Figure 1b. First, the 400-nm pump light, which lies within the ground-state absorption spectrum, promotes P3HT from the S_0 to the S_1^* state, with which the S_0 state has a large Franck-Condon overlap. The initially prepared exciton is able to dissipate its energy by a combination of torsional relaxation and EET to relax to the lowest-lying excited state, S_1 . The 1050-nm probe light (probe 1), which is located near the maximum of the ESA band, monitors the transitions from S_1 to higher-lying states, investigating the behavior of these states.

The black, solid curve shown in Figure 2a is the best-fit curve of the pump-probe data using a multi-exponential function of the form $f(t) = \sum_n A_n e^{-t/\tau_n}$ where, for each component, τ_n is the time constant and A_n is the amplitude. The best-fit values are shown in Table 1. First, the pump-probe result shows a rapid appearance of the excited-state absorption band immediately after excitation on a time scale near the instrument response function of approximately 150 fs. An additional, slower rise in the signal level with a time constant of 2.4 ps is also present. Furthermore, the result also shows decay components with time constants of 135 ps and 530 ps. The 530 ps time constant, which was fixed in the curve fitting analysis, is the characteristic lifetime of the P3HT exciton, as is discussed above.

The rising and decaying components of the pump-probe result indicate the following. First,

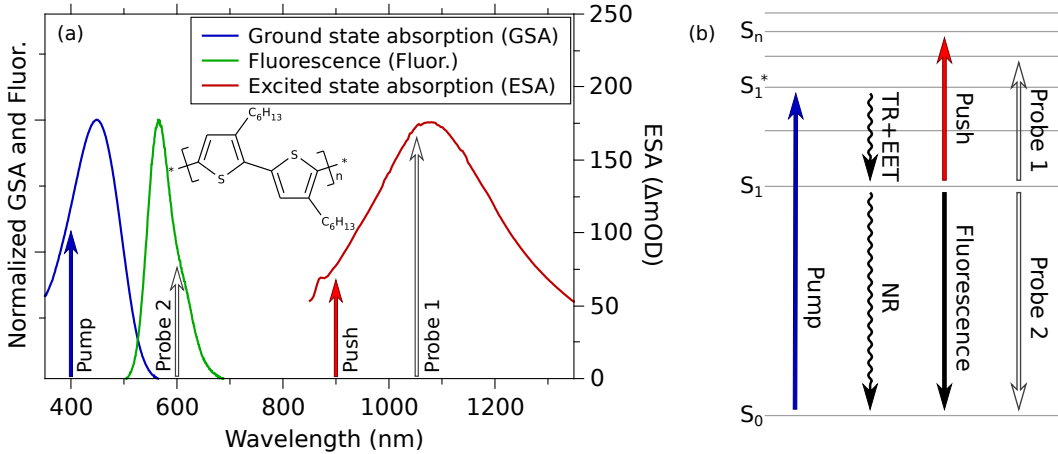


Figure 1: (a) Ground-state absorption, fluorescence and excited-state absorption spectra of dilute P3HT in THF. The pump, push, probe 1 and probe 2 wavelengths of 400 nm, 900 nm, 1050 nm and 600 nm, respectively, are indicated with arrows. Inset shows the structure of P3HT. (b) An energy diagram showing the photophysical processes involved in this study. Note that intersystem crossing is not shown and the push pulse is only present in the pump-push-probe experiment. TR: torsional relaxation, EET: excitonic energy transfer, NR: non-radiative deactivation.

Table 1: Fitting parameters for the pump-probe (ΔOD) and pump-push-probe ($\Delta\Delta OD$) data with $\lambda_{\text{push}} = 900 \text{ nm}$.^a

expt.	λ_{probe} (nm)	A_1 ^b	τ_1 (ps)	A_2	τ_2 (ps)	A_3	τ_3 (ps)	A_4	τ_4 (ps)
ΔOD	1050	–	–	–0.19	2.4	0.14	135	0.66	530 ^c
ΔOD	600	–	–	0.18	2.1	–0.22	60	–0.60	530 ^c
$\Delta\Delta OD$	1050	–0.80	0.16	–0.09	2.4	–0.07	135 ^d	–0.04	530 ^c
$\Delta\Delta OD$	600	0.86	0.16	0.08	2.8	0.03	109	0.03	530 ^c

^a The ΔOD and $\Delta\Delta OD$ data was fit to a multi-exponential function $f(t) = \sum_n A_n e^{-t/\tau_n}$. All parameters have a relative error of 15%. ^b $\sum_n |A_n| = 1$. ^c Fixed to value obtained from fluorescence lifetime measurements. ^d Fixed to value obtained from pump-probe experiment.

the 2.4 ps rising component, τ_2 , is the result of a significant red-shift of the excited-state absorption band up to 1050 nm at early time, as shown in Supporting Information. This red-shift is due to rapid energy dissipation of the initially prepared excited state. The general agreement from a number of studies is that either torsional reorganization, EET, or both are responsible for these rapid dynamics. Banerji et al. used a global analysis of multicolor fluorescence upconversion data to reconstruct the time-resolved fluorescence spectra of P3HT and concluded that self-localization of excitons occurs approximately 100 fs following the photoexcitation event.¹⁹ Furthermore, Wells and Blank demonstrated that highly correlated relaxation of P3HT excitons occurs at

$t < 200 \text{ fs}$.²⁵ The observed dynamic Stokes shift is the result of exciton self trapping mediated by low-frequency torsional modes of P3HT. Recently, Busby et al. used broadband pump-probe and pump-dump-probe spectroscopy to investigate the early-time dynamics of P3HT.³⁰ They concluded that small-amplitude torsional reorganization (planarization) of the thiophene units take place at $t < 1 \text{ ps}$, while large-amplitude motions occur at $t > 1 \text{ ps}$. While the long time constant, $\tau_4 = 530 \text{ ps}$, represents the exciton lifetime,^{19,22,23} the process with an intermediate time constant ($\tau_3 = 135 \text{ ps}$) is attributable to additional slow torsional relaxation.^{19,24,30,37–40}

Figure 2a also shows the ΔOD at 1050 nm as a function of pump-probe time delay in the

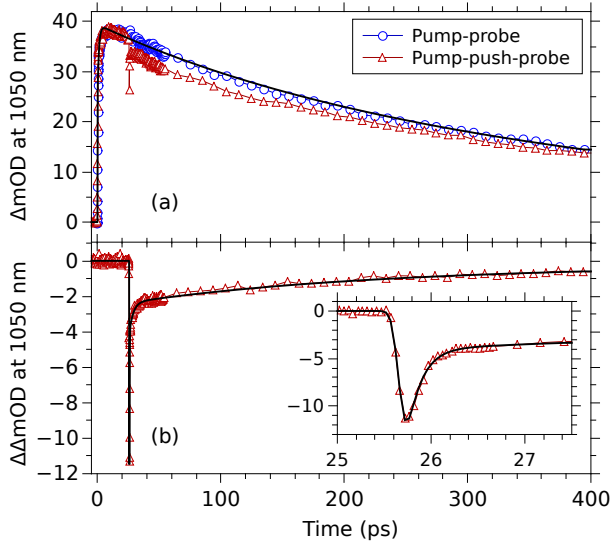


Figure 2: (a) The dynamics of the exciton-induced absorption at 1050 nm in the pump-probe (blue circles) and pump-push-probe experiments (red triangles). (b) The change in ΔOD ($\Delta\Delta OD$) due to the push pulse. Fit curves are indicated as solid black curves.

pump-push-probe experiment (red triangles). The pump beam is modulated while the 900-nm push beam is on at all times. The arrival time of the push pulse in the pump-push-probe experiment is 25.8 ps after the pump pulse, which enables the exciton to be sufficiently relaxed before being excited by the push pulse. In this experiment, the exciton is generated in an identical fashion to the pump-probe experiment. However, after the exciton has undergone relaxation to the S_1 state, it is re-excited by the push pulse to a higher-lying state, S_n . The photophysical events in the pump-push-probe experiment are shown in Figure 1b. As a result, probing the ESA band as a function of time offers insight into the S_n to S_1 relaxation.

On introduction of the push pulse, the pump-push-probe result shows a significant deviation from the pump-probe transient, as shown in Figure 2a. The ΔOD signal at 1050 nm is depleted by approximately 30%, which is a direct measure of the level of excitons promoted by the push pulse to the S_n state. We have also performed a power dependence study of the push pulse while keeping the pump power constant. The results, which are found in Supporting Information, show that the depletion

of the ΔOD signal at 1050 nm signal is linear with respect to the range of push powers used in this study. The majority of the ΔOD signal exhibits a rapid recovery, indicating the subsequent relaxation of excitons from the S_n state to the S_1 state. A portion of the signal shows an incomplete recovery over the duration of the experiment, which results in the signal difference in Figure 2a at $t > 25.8$ ps. Our analysis indicates that this signal difference is due to exciton dissociation by the push pulse to form free carriers, which is discussed below.

The effect of the push is highlighted in Figure 2b, which shows the change in ΔOD , *i.e.*, $\Delta\Delta OD$. In other words, the data in Figure 2b is the difference between the two traces shown in Figure 2a, as follows.

$$\Delta\Delta OD(\lambda, t) = \Delta OD(\lambda, t)_{\text{push on}} - \Delta OD(\lambda, t)_{\text{push off}} \quad (1)$$

Experimentally, this signal is acquired by modulating the push pulse while keeping the pump pulse on at all times. It is important to note that this simple light modulating arrangement instead of a more elaborate one employed in other studies^{30,33} is used here because the push pulse only exhibits an optical response in the presence of the pump light, as shown in Supporting Information. In other words, the push-probe signal is negligible. It is noted that two-photon excitation of P3HT may be possible as the energy of two push photons overlaps with the linear absorption band of P3HT. However, the push peak intensity used in our study (12.7 GWcm^{-2}) is ~ 30 times lower than that used in a study involving two-photon excitation of P3HT.⁴¹ Hence, the negligible optical response by the push pulse alone is expected.

Figure 2b shows that the depletion of the $\Delta\Delta OD$ signal at $t = 25.8$ ps is followed by a fast recovery over a period of several picoseconds. In addition, it is apparent that there is a portion of the signal that fails to recover completely within the experimental time window. Four exponential decay components are used to fit the $\Delta\Delta OD$ data. The longest time constants τ_3 – τ_4 are fixed at 135 ps and 530 ps, corresponding to the decay components in the pump-probe experiment as discussed above. The identical τ_3

and τ_4 values for these two sets of data are chosen on the grounds that apart from the early-time push pulse-associated dynamics, the decaying ΔOD signal with the push pulse (red curve in Figure 2a) is simply a portion of that without the push pulse, which can be shown using eq 1. In this case, the ΔOD signal with the push pulse is 11% lower than that without it (Figure 2a), indicating that the same percentage of the total exciton population is unrecovered after excitation by the push pulse. We argue that the “missing” excitons as a result of the push pulse-excitation are attributable to exciton dissociation to generate charge carriers in P3HT, consistent with the observation in a previous pump-push-probe study on a different conjugated polymer.³⁴

It is important to note that in the event of exciton dissociation to form charge carriers, namely the electron and hole-polaron, they are expected to undergo rapid geminate recombination to yield ground-state P3HT because of the close proximity of the charged species.⁴² Because the dissociated excitons do not relax back to the S_1 state, this phenomenon manifests as a persistent, negative $\Delta\Delta\text{OD}$ signal such as that shown in Figure 2b. Therefore, it follows that exciton dissociation should result in a corresponding positive $\Delta\Delta\text{OD}$ signal in the spectral region where ground-state P3HT absorbs due to charge recombination. Indeed such a signal is present in our experiment and shown in Supporting Information. The magnitude of this positive $\Delta\Delta\text{OD}$ signal is a function of the ground-state absorbance, the level of exciton produced in the photoexcitation event by the pump pulse, the proportion of excitons promoted by the push pulse and the proportion of the unrecovered excitons. Calculation of the expected value for the positive $\Delta\Delta\text{OD}$ signal at 465 nm is shown in Supporting Information. The magnitude of the observed $\Delta\Delta\text{OD}$ signal and the expected value show excellent agreement and hence the assignment of the unrecovered $\Delta\Delta\text{OD}$ signal in the presence of the push pulse to exciton dissociation is strongly supported. Pump-push-probe experiments were also carried out using $\lambda_{\text{push}} = 1200$ nm and the results are shown in Supporting Information.

It is interesting that the $\Delta\Delta\text{OD}$ dynamics are nearly identical to those with $\lambda_{\text{push}} = 900$ nm. The lack of dependence of the dynamics on push pulse wavelength has implications on the exciton binding energy and is discussed below. With regards to the “missing” excitons, we have also considered that the negative $\Delta\Delta\text{OD}$ signal as shown in Figure 2b may be due to stimulated deactivation of the exciton by the push pulse. However, this alternative explanation is highly unlikely because the push pulse, which has a wavelength of 900 nm or longer, is sufficiently detuned from any emission wavelengths of P3HT excitons such that stimulated deactivation is expected to be negligible. In short, exciton dissociation by the push pulse is significantly more likely. We have also considered that the persistent $\Delta\Delta\text{OD}$ signal in Figure 2b may be due to production of triplet excitons as a consequence of charge carrier recombination. Although our ΔOD data show the presence of triplet excitons, which manifests as a long-lived induced absorption band at 820 nm,²³ it is unclear if triplet excitons play a significant role in the $\Delta\Delta\text{OD}$ data at the same wavelength (Supporting Information). However, the dynamics and magnitude of the positive $\Delta\Delta\text{OD}$ signal at 465 nm indicate that the ground state recovery is complete within picoseconds, which is significantly shorter than the triplet exciton lifetime of hundreds of nanoseconds.²³ Therefore, we believe the contribution of triplet states is insignificant.

To our knowledge, these results are the first observation of exciton dissociation to generate short-lived charge carriers in a conjugated polymer in solution, in which the generation and recombination of charges are confined on a single chain. A number of studies have reported generation of charge carriers in neat polymer films due to photoexcitation.^{23,34,43–47} In particular, Cook et al. have reported generation of charge carriers in a P3HT thin-film.²³ By analyzing their kinetic results, they concluded that generation of polarons is an early-time photo-induced event, which takes place prior to the emission of the singlet exciton. While a portion of the charge carriers in films are able to overcome geminate recombination due to suffi-

ciently high charge mobility, the charge carriers in single P3HT chains are confined on the polymer chains and hence are able to undergo rapid geminate recombination. Ultrafast geminate recombination of charges on a conjugated polymer provides a valuable measure of the yield of charge generation due to re-excitation of excitons by the push pulse. As mentioned above, the negative $\Delta\Delta\text{OD}$ signal at the push pulse-arrival time in Figure 2b indicates excitation of the exciton and the long-lived signal reflects the depletion of excitons due to geminate recombination. As a result, the yield of charge generation can be calculated by taking the ratio between the amplitudes of the two signals. In this case, using the $\Delta\Delta\text{OD}$ results with $\lambda_{\text{probe}} = 1050$ nm in Table 1, the yield of charge generation is therefore $(|A_3| + |A_4|) / \sum_n |A_n|$, which has a value of $\sim 11\%$. As mentioned above, Gadermaier et al. used pump-push-probe spectroscopy to investigate a thin film of methyl-substituted ladder-type poly(para)phenyl.³⁴ An important conclusion from their study is that the charge carrier generation has a strong push arrival time-dependence. Their results show a maximum charge carrier yield at a pump-push delay of ~ 0.3 ps, which is followed by a significant decrease such that a negligible yield is present at a pump-push delay of ≥ 3 ps. In this study, we have also investigated the dependence of charge carrier generation on the pump-push time delay in which delays ranging from 0.25 to 500 ps were used. Interestingly, no dependence on the pump-push delay was observed. As shown in Supporting Information, throughout the entire lifetime of the exciton the push pulse consistently results in dissociation of $\sim 11\%$ of the high-energy exciton population to yield charge carriers. The dependence of charge carrier generation yield on the pump pulse delay time is possibly related to the early-time dynamics of the polymer. It is known that methyl-substituted ladder-type poly(para)phenyl undergoes vibrational cooling in the first few picoseconds upon photoexcitation and during which time “hot” excitons can be dissociated effectively to form charge carriers.³⁴ In contrast, early-time dynamics of P3HT are related to torsional relaxation.^{24,30}

It is conceivable that a significant portion of P3HT excitons are nearly fully relaxed even at the earliest pump-push delay in our study, especially because a recent study shows that ultrafast torsional relaxation occurs on a time scale of ~ 100 fs.³² As a consequence, a negligible dependence of charge carrier generation on the pump-push delay is present for P3HT.

The results on charge carrier generation suggest that the exciton binding energy of single P3HT chains in tetrahydrofuran is approximately 1.03 eV or lower, because we have used a λ_{push} as long as 1200 nm, as shown in Supporting Information. Studies have shown that the exciton binding energy of isolated chains is typically 2 to 3 eV.^{48–50} However, it must be noted that these results are based on theoretical modelling on single polymer chains alone, *i.e.*, in the absence of any solvent. Furthermore, these studies showed that in a polymer film, owing to a significant level of interchain coupling, dielectric screening of conjugated polymers results in the decrease of exciton binding energy to ~ 1 eV. It is well established by experimental measurements that the exciton binding energy in P3HT films is ≤ 1 eV.⁵¹ For several other conjugated polymers including MEH-PPV, PFO and P3OT, the exciton binding energies of the films are even lower, ranging from 0.3 to 0.6 eV.⁵² Therefore, it is clear that the presence of a dielectric medium, *e.g.*, a solvent such as THF, around the conjugated polymer can lower the exciton binding energy. It is interesting that in a study where electrolytes were added to poly-2,7-(9,9-dihexylfluorene) in THF, an exciton binding energy of 0.2 eV was measured.⁵³ Overall, the ≤ 1 eV exciton binding energy from this study shows good agreement with previous studies.

The two remaining decay components in the $\Delta\Delta\text{OD}$ data, with time constants τ_1 and τ_2 of 0.16 ps and 2.4 ps, respectively, are present as a result of the transition from S_n to S_1 . A recent study by Clark et al. offers important insight into the ultrafast non-radiative transition from S_n to S_1 .³² By examining oligofluorenes in solution using pump-push-probe spectroscopy, these authors observed a dynamic component in their data with a sub-0.1 ps time constant.

Using non-adiabatic excited-state molecular dynamics to model their data, Clark et al. concluded that oligofluorenes can undergo a conformation change on this ultrafast time scale, which is analogous to inertial solvation observed in the 1990s.⁵⁴⁻⁵⁶ Therefore, in our study it is reasonable to assign the decay component with a time constant of 0.16 ps time to ultrafast torsional relaxation. The slower component with a time constant of 2.4 ps can be assigned to larger amplitude and further torsional relaxation, which has been observed in previous studies.^{24,30} It is interesting that the decay time constants and relative amplitudes of these two relaxation components are independent of the pump-push delay time (Supporting Information). These results indicate that the relaxation dynamics of the S_n state are insensitive to whether the original S_1 is a torsionally “hot” or “cool” exciton. This outcome is particularly interesting especially with long pump-push delay times, *e.g.*, 500 ps. In this case, it is reasonable to assume that the S_1 state is fully relaxed, with the singlet exciton localized on a chromophoric segment with a significant conjugation length. In the event that relocalization of the push pulse-induced high-energy exciton occurs within the same conjugated segment, the S_n to S_1 relaxation is expected to be free of the larger amplitude torsional relaxation. However, the presence of the decay component with a 2.4 ps time constant at all pump-push delay times suggests that the push pulse induces a high level of exciton delocalization, allowing it to relocalize and undergo relaxation in a different segment of the polymer chain not previously excited by the pump pulse.

Figure 3 shows the results of repeating the pump-probe and pump-push-probe experiments, but probing the SE band at 600 nm. Figures 3a and 3b show the data from the ΔOD and $\Delta\Delta OD$ experiments, respectively. The data appear to mirror that obtained from probing the ESA band (Figure 2), which is expected as both are the result of transitions originating from the same electronic state. The similarity of the ESA and SE dynamics is confirmed in the fitting parameters (Table 1) where the equivalent components are seen in both

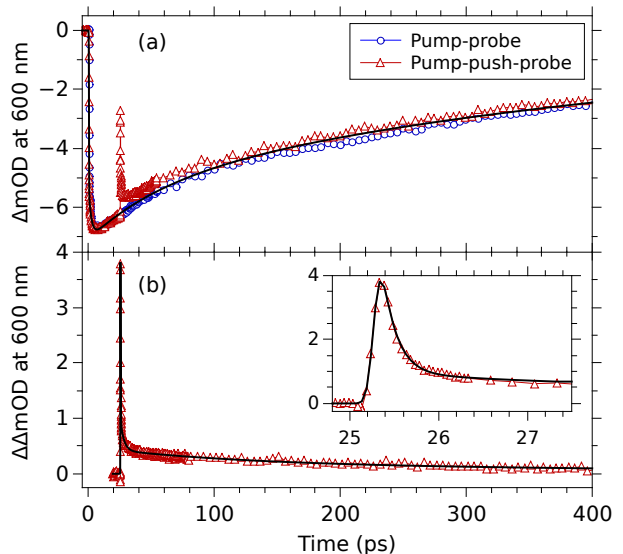


Figure 3: The dynamics of stimulated emission at 600 nm in the pump-probe (a, blue circles) and pump-push-probe experiments (a, red triangles). The change in ΔOD due to the push pulse is shown in (b). Fit curves are indicated with black lines.

the pump-probe and pump-push-probe experiments. A subtle difference between the ESA and SE data is the magnitude of the sub-picosecond recovery component. This difference can be seen in Figures 2a and 3a as the extent of the deviation in the signal due to the push pulse. As ΔOD is an indication of the population of excitons, $\Delta\Delta OD/\Delta OD$ at the push pulse arrival time should be a measure of the proportion of excitons being affected by the push pulse, and should be identical for both the ESA and SE data. This is not the case however, with this proportion being $\sim 30\%$ for the ESA and $\sim 50\%$ for the SE data. The difference can be attributed to dissociation of the exciton into an electron and hole-polaron. The hole-polaron has been observed previously in transient absorption studies of P3HT films, nanoparticles and nanowires, exhibiting an absorption peak overlapping the red-side of the emission.^{13,23,36,57} A short-lived hole-polaron absorption induced by the push would manifest as a positive $\Delta\Delta OD$ signal. As a consequence of the overlap between this positive signal and the negative signal of the SE band, an apparently larger than normal de-

crease in SE due to the push is observed. The ESA data are free from the same effect, as the hole-polaron absorption does not overlap the ESA band. This observation provides further support that the push pulse is causing dissociation of the exciton and production of charge carrier states.

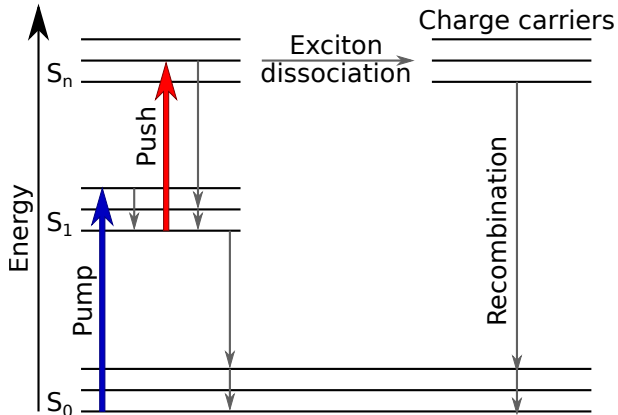


Figure 4: Energy level diagram showing the initial excitation by the pump pulse to produce the singlet exciton. The push pulse promotes the exciton to a high-energy, delocalized state which allows dissociation to produce charge carriers.

Figure 4 summarizes the pump-push-probe results in this study. The pump vertically excites the polymer to form a delocalized singlet exciton which rapidly localizes to a section of the polymer within ~ 100 fs to give the S₁ state. Torsional motion between the thiophene rings acts to increase the planarization of the polymer section, lowering the energy of the exciton. Through the process of EET, the exciton may hop to nearby, lower energy regions of the chain, which themselves can undergo further relaxation due to torsional motion. The arrival of the push pulse then further excites the exciton, producing a high-energy, delocalized state, S_n. From the highly excited state, several relaxation pathways are available. The majority of the high-energy excitons rapidly decay back to the original S₁ state, possibly localizing in a new, previously unvisited conjugated segment of the polymer on a time scale of ~ 160 fs, which corresponds to the fastest decay time constant observed in this study. This assignment shows agreement with the expected

lifetime of the S_n state of ~ 250 fs, which is calculated using the gap law.^{34,58} The energy gap between the S₁ and S_n state is estimated using the peak wavelength of the ESA band of 1075 nm. The delocalization of the high-energy exciton also provides the opportunity for exciton dissociation to produce charge carrier states (electron and hole-polaron). Owing to the presence of charge carriers on the same polymer chain, geminate recombination occurs rapidly, returning the polymer to the S₀ ground-state.

The rate constant of exciton dissociation, k_{ED} , may be calculated using the yield of exciton dissociation, Φ_{ED} , and the lifetime of the S_n state, τ_{S_n} and eq 2.

$$\Phi_{ED} = \frac{k_{ED}}{1/\tau_{S_n}} \quad (2)$$

Values of 11% and 160 fs are used for Φ_{ED} and τ_{S_n} , respectively. The calculated k_{ED} has a value of ~ 0.67 ps⁻¹, which corresponds to an exciton dissociation time constant, τ_{ED} , of ~ 1.5 ps. The $\Delta\Delta OD$ data at a wavelength under the ground-state absorption spectrum (Supporting Information), which reports the recovery of the ground-state due to geminate recombination of charge carriers produced during exciton dissociation, shows an increase on a time scale consistent with τ_{ED} . This result indicates that geminate recombination occurs significantly faster than exciton dissociation, which is expected given the close proximity of charge carriers on the polymer chain.

In conclusion, we have used pump-push-probe spectroscopy to show that excitons on isolated P3HT chains in solution may be delocalized by the use of a secondary photoexcitation, a push pulse. Of these high-energy excitons, $\sim 11\%$ were found to dissociate into charge carriers, with the remainder having the possibility of relocalizing on a different region of the polymer chain. Exciton dissociation is present with a push wavelength up to 1200 nm, giving a value for the binding energy of the exciton of ≤ 1 eV. The lack of time dependence of the pump-push delay indicates that ultrafast torsional relaxation causes the majority of relaxation of the P3HT exciton on a time scale of ≤ 160 fs.

Experimental Section

Materials and sample preparation. Regioregular P3HT (MW = 50 000 g mol⁻¹, 99% regioregular, Rieke Metals) was dissolved in freshly distilled THF (reagent grade, Scharlau) using sonication at 25 °C for one hour to produce 0.1 g L⁻¹ solutions, which were then filtered through a 0.2 µm nylon filter.

Steady state spectroscopy. The steady-state absorption spectrum was obtained using a P3HT solution diluted to 0.01 g L⁻¹ using a quartz cuvette with a 1 cm pathlength and a Cary 300 UV-visible absorption spectrophotometer. The fluorescence spectrum was obtained on a Perkin-Elmer LS-55 fluorescence spectrometer with the same sample used for the steady-state absorption measurement. Excitation wavelength was 400 nm and excitation and emission slit widths set at 5 nm.

Pump-probe and pump-push-probe spectroscopy. Schematic diagram of the pump-probe/pump-push-probe transient absorption apparatus are supplied in Supporting Information. All laser pulses originated from a Ti:sapphire regenerative amplifier (Spectra-Physics, Spitfire Pro XP 100F) producing 100 fs pulses at a repetition rate of 1 kHz centered at 800 nm. Pump pulses at 400 nm were generated by frequency doubling of the fundamental output using a 0.5 mm BBO crystal. The pump pulse energy was 1.8 µJ with a spot size of 700 µm. Push pulses at 900 nm or 1200 nm were produced using an optical parametric amplifier (Light Conversion, TOPAS-C) with a pulse energy of 1.8 µJ and a spot size of 475 µm. An optical chopper was used to mechanically modulate either the pump or push beams at a frequency of 500 Hz to obtain the ΔOD or $\Delta\Delta OD$ values, respectively. A white light continuum was generated for probe pulses by a 3.2 mm thick sapphire crystal for the 600 nm probe light and a 12.7 mm thick sapphire crystal for the 1050 nm probe light, with the arrival time determined by a computer controlled delay line. The probe was split into signal and reference beams and fed to a pair of linear de-

tectors. CMOS sensors were used for the visible (Ultrafast Systems, CAM-VIS-2) and In-GaAs diode arrays for the near-IR (Ultrafast Systems, CAM-NIR) wavelengths. Probe spot sizes were 260 µm for the visible and 75 µm for the near-IR, with the energy of the pulses always much less than those of the pump and push pulses. Relative to the probe, the pump and push beam crossing angles were 5° and -4° respectively, with polarizations set at the magic angle of 54.7°. Samples had a concentration of 0.02 g L⁻¹ for the visible and 0.1 g L⁻¹ for the near-IR experiments and were studied in a quartz cuvette with a 2 mm path length (Starna Cells 21-Q-2) with continuous stirring. By changing the sample after each run of the experiments, each sample was subjected to less than 90 minutes of laser exposure and effects of photobleaching was not observed to exceed 10%. Fitting of the data was performed using a Gaussian instrument response function of 150 fs (FWHM).

Acknowledgement The authors acknowledge Mr Scott N. Clifton for his assistance in experiment and data analysis, Dr David M. Huang for stimulating discussion, and the Australian Research Council for funding support (LE0989747).

Supporting Information Available

The following files are available free of charge. Additional figures, calculations, tables of fitting parameters and details of experimental procedures.

References

- (1) Brabec, C.; Sariciftci, N.; Hummelen, J. Plastic Solar Cells. *Adv. Funct. Mater.* **2001**, *11*, 15–26.
- (2) Li, G.; Shrotriya, V.; Huang, J.; Yao, Y.; Moriarty, T.; Emery, K.; Yang, Y. High-Efficiency Solution Processable Polymer Photovoltaic Cells by Self-Organization of

- Polymer Blends. *Nat. Mater.* **2005**, *4*, 864–868.
- (3) Guenes, S.; Neugebauer, H.; Sariciftci, N. S. Conjugated Polymer-Based Organic Solar Cells. *Chem. Rev.* **2007**, *107*, 1324–1338.
 - (4) Thompson, B. C.; Fréchet, J. M. J. Organic Photovoltaics — Polymer-Fullerene Composite Solar Cells. *Angew. Chem., Int. Ed.* **2008**, *47*, 58–77.
 - (5) Chen, T.-A.; Wu, X.; Rieke, R. D. Regiocontrolled Synthesis of Poly(3-alkylthiophenes) Mediated by Rieke Zinc: Their Characterization and Solid-State Properties. *J. Am. Chem. Soc.* **1995**, *117*, 233–244.
 - (6) Spano, F. C. The Spectral Signatures of Frenkel Polarons in H- and J-Aggregates. *Acc. Chem. Res.* **2009**, *43*, 429–439.
 - (7) Kim, J. S.; Lee, J. H.; Park, J. H.; Shim, C.; Sim, M.; Cho, K. High-Efficiency Organic Solar Cells Based on Preformed Poly(3-hexylthiophene) Nanowires. *Adv. Funct. Mater.* **2011**, *21*, 480–486.
 - (8) Schwarz, K. N.; Kee, T. W.; Huang, D. M. Coarse-Grained Simulations of the Solution-Phase Self-Assembly of Poly(3-hexylthiophene) Nanostructures. *Nanoscale* **2013**, *5*, 2017–2027.
 - (9) Samitsu, S.; Shimomura, T.; Heike, S.; Hashizume, T.; Ito, K. Effective Production of Poly(3-alkylthiophene) Nanofibers by means of Whisker Method using Anisole Solvent: Structural, Optical, and Electrical Properties. *Macromolecules* **2008**, *41*, 8000–8010.
 - (10) Martin, T. P.; Wise, A. J.; Busby, E.; Gao, J.; Roehling, J. D.; Ford, M. J.; Larsen, D. S.; Moulé, A. J.; Grey, J. K. Packing Dependent Electronic Coupling in Single Poly(3-hexylthiophene) H- and J-Aggregate Nanofibers. *J. Phys. Chem. B* **2012**, *117*, 4478–4487.
 - (11) Li, H.; Li, J.; Xu, Q.; Hu, X. Poly(3-hexylthiophene)/TiO₂ Nanoparticle-Functionalized Electrodes for Visible Light and Low Potential Photoelectrochemical Sensing of Organophosphorus Pesticide Chlpyrifos. *Anal. Chem.* **2011**, *83*, 9681–9686.
 - (12) Hu, Z.; Gesquiere, A. J. Charge Trapping and Storage by Composite P3HT/PC₆₀BM Nanoparticles Investigated by Fluorescence-Voltage/Single Particle Spectroscopy. *J. Am. Chem. Soc.* **2011**, *133*, 20850–20856.
 - (13) Clifton, S. N.; Huang, D. M.; Massey, W. R.; Kee, T. W. Femtosecond Dynamics of Excitons and Hole-Polarons in Composite P3HT/PCBM Nanoparticles. *J. Phys. Chem. B* **2013**, *117*, 4626–4633.
 - (14) Lee, S.-H.; Kim, D.-H.; Kim, J.-H.; Lee, G.-S.; Park, J.-G. Effect of Metal-Reflection and Surface-Roughness Properties on Power-Conversion Efficiency for Polymer Photovoltaic Cells. *J. Phys. Chem. C* **2009**, *113*, 21915–21920.
 - (15) Dang, M. T.; Hirsch, L.; Wantz, G. P3HT:PCBM, Best Seller in Polymer Photovoltaic Research. *Adv. Mater.* **2011**, *23*, 3597–3602.
 - (16) Lee, S.-H.; Kim, J.-H.; Shim, T.-H.; Park, J.-G. Effect of Interface Thickness on Power Conversion Efficiency of Polymer Photovoltaic Cells. *Electron. Mater. Lett.* **2009**, *5*, 47–50.
 - (17) Marsh, R. A.; Hodgkiss, J. M.; Albert-Seifried, S.; Friend, R. H. Effect of Annealing on P3HT:PCBM Charge Transfer and Nanoscale Morphology Probed by Ultrafast Spectroscopy. *Nano Lett.* **2010**, *10*, 923–930.
 - (18) Kirkpatrick, J.; Keivanidis, P. E.; Bruno, A.; Ma, F.; Haque, S. A.; Yarstev, A.; Sundstrom, V.; Nelson, J. Ultrafast Transient Optical Studies

- of Charge Pair Generation and Recombination in Poly-3-Hexylthiophene (P3HT):[6,6]Phenyl C₆₁ Butyric Methyl Acid Ester (PCBM) Blend Films. *J. Phys. Chem. B* **2011**, *115*, 15174–15180.
- (19) Banerji, N.; Cowan, S.; Vauthey, E.; Heeger, A. J. Ultrafast Relaxation of the Poly(3-hexylthiophene) Emission Spectrum. *J. Phys. Chem. C* **2011**, *115*, 9726–9739.
- (20) Chen, K.; Barker, A. J.; Reish, M. E.; Gordon, K. C.; Hodgkiss, J. M. Broadband Ultrafast Photoluminescence Spectroscopy Resolves Charge Photogeneration via Delocalized Hot Excitons in Polymer:Fullerene Photovoltaic Blends. *J. Am. Chem. Soc.* **2013**, *135*, 18502–18512.
- (21) Ferreira, B.; da Silva, P. F.; Seixas de Melo, J. S.; Pina, J.; Maçanita, A. Excited-State Dynamics and Self-Organization of Poly(3-hexylthiophene) (P3HT) in Solution and Thin Films. *J. Phys. Chem. B* **2012**, *116*, 2347–2355.
- (22) Wells, N. P.; Boudouris, B. W.; Hillmyer, M. A.; Blank, D. A. Intramolecular Exciton Relaxation and Migration Dynamics in Poly(3-hexylthiophene). *J. Phys. Chem. C* **2007**, *111*, 15404–15414.
- (23) Cook, S.; Furube, A.; Katoh, R. Analysis of the Excited States of Regioregular Polythiophene P3HT. *Energ. Environ. Sci.* **2008**, *1*, 294–299.
- (24) Parkinson, P.; Muller, C.; Stingelin, N.; Johnston, M. B.; Herz, L. M. Role of Ultrafast Torsional Relaxation in the Emission from Polythiophene Aggregates. *J. Phys. Chem. Lett.* **2010**, *1*, 2788–2792.
- (25) Wells, N. P.; Blank, D. A. Correlated Exciton Relaxation in Poly(3-hexylthiophene). *Phys. Rev. Lett.* **2008**, *100*, 086403.
- (26) Guo, J.; Ohkita, H.; Yokoya, S.; Benten, H.; Ito, S. Bimodal Polarons and Hole Transport in Poly(3-hexylthiophene):Fullerene Blend Films. *J. Am. Chem. Soc.* **2010**, *132*, 9631–9637.
- (27) Grancini, G.; Maiuri, M.; Fazzi, D.; Petrozza, A.; Egelhaaf, H.-J.; Brida, D.; Cerullo, G.; Lanzani, G. Hot Exciton Dissociation in Polymer Solar Cells. *Nat. Mater.* **2013**, *12*, 29–33.
- (28) Gélinas, S.; Rao, A.; Kumar, A.; Smith, S. L.; Chin, A. W.; Clark, J.; van der Poll, T. S.; Bazan, G. C.; Friend, R. H. Ultrafast Long-Range Charge Separation in Organic Semiconductor Photovoltaic Diodes. *Science* **2014**, *343*, 512–516.
- (29) Kaake, L. G.; Moses, D.; Heeger, A. J. Coherence and Uncertainty in Nanostructured Organic Photovoltaics. *J. Phys. Chem. Lett.* **2013**, *4*, 2264–2268.
- (30) Busby, E.; Carroll, E. C.; Chinn, E. M.; Chang, L.; Moule, A. J., A. J.e; Larsen, D. S. Excited-State Self-Trapping and Ground-State Relaxation Dynamics in Poly(3-hexylthiophene) Resolved with Broadband Pump-Dump-Probe Spectroscopy. *J. Phys. Chem. Lett.* **2011**, *2*, 2764–2769.
- (31) Collini, E.; Scholes, G. D. Coherent Intra-chain Energy Migration in a Conjugated Polymer at Room Temperature. *Science* **2009**, *323*, 369–373.
- (32) Clark, J.; Nelson, T.; Tretiak, S.; Cirimi, G.; Lanzani, G. Femtosecond Torsional Relaxation. *Nat. Phys.* **2012**, *8*, 225–231.
- (33) Bakulin, A. A.; Rao, A.; Pavelyev, V. G.; van Loosdrecht, P. H. M.; Pshenichnikov, M. S.; Niedzialek, D.; Cornil, J.; Beljonne, D.; Friend, R. H. The Role of Driving Energy and Delocalized States for Charge Separation in Organic Semiconductors. *Science* **2012**, *335*, 1340–1344.
- (34) Gadermaier, C.; Cerullo, G.; Sansone, G.; Leising, G.; Scherf, U.; Lanzani, G. Time-Resolved Charge Carrier Generation from

- Higher Lying Excited States in Conjugated Polymers. *Phys. Rev. Lett.* **2002**, *89*, 117402.
- (35) Kraabel, B.; Moses, D.; Heeger, A. J. Direct Observation of the Intersystem Crossing in Poly(3-octylthiophene). *J. Chem. Phys.* **1995**, *103*, 5102–5108.
- (36) Guo, J.; Ohkita, H.; Bente, H.; Ito, S. Near-IR Femtosecond Transient Absorption Spectroscopy of Ultrafast Polaron and Triplet Exciton Formation in Polythiophene Films with Different Regioregularities. *J. Am. Chem. Soc.* **2009**, *131*, 16869–16880.
- (37) Westenhoff, S.; Beenken, W. J. D.; Friend, R. H.; Greenham, N. C.; Yartsev, A.; Sundström, V. Anomalous Energy Transfer Dynamics due to Torsional Relaxation in a Conjugated Polymer. *Phys. Rev. Lett.* **2006**, *97*, 166804.
- (38) Hwang, I.; Scholes, G. D. Electronic Energy Transfer and Quantum-Coherence in Conjugated Polymers. *Chem. Mater.* **2011**, *23*, 610–620.
- (39) Adachi, T.; Lakhwani, G.; Traub, M. C.; Ono, R. J.; Bielawski, C. W.; Barbara, P. F.; Vanden Bout, D. A. Conformational Effect on Energy Transfer in Single Polythiophene Chains. *J. Phys. Chem. B* **2012**, *116*, 9866–9872.
- (40) Yu, W.; Zhou, J.; Bragg, A. E. Exciton Conformational Dynamics of Poly(3-hexylthiophene) (P3HT) in Solution from Time-Resolved Resonant-Raman Spectroscopy. *J. Phys. Chem. Lett.* **2012**, *3*, 1321–1328.
- (41) Trotzky, S.; Hoyer, T.; Tuszynski, W.; Lienau, C.; Paris, J. Femtosecond Upconversion Technique for Probing the Charge Transfer in a P3HT:PCBM Blend via Photoluminescence Quenching. *J. Phys. D: Appl. Phys.* **2009**, *42*, 055105.
- (42) Gao, B.-R.; Wang, H.-Y.; Wang, H.; Yang, Z.-Y.; Wang, L.; Jiang, Y.; Hao, Y.-W.; Chen, Q.-D.; Sun, H.-B. Investigation of Polaron Pair Dynamics in Poly(3-hexylthiophene) Film by Time Resolved Spectroscopy. *IEEE J. Quantum. Electron.* **2012**, *48*, 425–432.
- (43) Stagira, S.; Nisoli, M.; Lanzani, G.; De Silvestri, S.; Cassano, T.; Tommasi, R.; Babudri, F.; Farinola, G. M.; Naso, F. Intrachain Charge Generation and Recombination in Alkoxy-Substituted Poly-(*p*-phenylenevinylene) Films. *Phys. Rev. B* **2001**, *64*, 205205.
- (44) Harrison, M. G.; Grüner, J.; Spencer, G. C. W. Analysis of the Photocurrent Action Spectra of MEH-PPV Polymer Photodiodes. *Phys. Rev. B* **1997**, *55*, 7831–7849.
- (45) Hendry, E.; Koeberg, M.; Schins, J. M.; Siebbeles, L. D. A.; Bonn, M. Ultrafast Charge Generation in a Semiconducting Polymer Studied with THz Emission Spectroscopy. *Phys. Rev. B* **2004**, *70*, 033202.
- (46) Miranda, P. B.; Moses, D.; Heeger, A. J. Ultrafast Photogeneration of Charged Polarons in Conjugated Polymers. *Phys. Rev. B* **2001**, *64*, 081201.
- (47) Moses, D.; Dogariu, A.; Heeger, A. J. Ultrafast Photoinduced Charge Generation in Conjugated Polymers. *Chem. Phys. Lett.* **2000**, *316*, 356–360.
- (48) Moore, E. E.; Yaron, D. An Explicit-solvent Dynamic-Dielectric Screening Model of Electron-Hole Interactions in Conjugated Polymers. *J. Chem. Phys.* **1998**, *109*, 6147–6156.
- (49) van der Horst, J.-W.; Bobbert, P. A.; de Jong, P. H. L.; Michels, M. A. J.; Brocks, G.; Kelly, P. J. Ab Initio Prediction of the Electronic and Optical Excitations in Polythiophene: Isolated Chains Versus Bulk Polymer. *Phys. Rev. B* **2000**, *61*, 15817–15826.

- (50) Barford, W.; Bursill, R. J.; Yaron, D. Dynamical Model of the Dielectric Screening of Conjugated Polymers. *Phys. Rev. B* **2004**, *69*, 155203.
- (51) Deibel, C.; Mack, D.; Gorenflot, J.; Schöll, A.; Krause, S.; Reinert, F.; Rauh, D.; Dyakonov, V. Energetics of Excited States in the Conjugated Polymer Poly(3-hexylthiophene). *Phys. Rev. B* **2010**, *81*, 085202.
- (52) Knupfer, M. Exciton Binding Energies in Organic Semiconductors. *Appl. Phys. A* **2003**, *77*, 623–626.
- (53) Takeda, N.; Asaoka, S.; Miller, J. R. Nature and Energies of Electrons and Holes in a Conjugated Polymer, Polyfluorene. *J. Am. Chem. Soc.* **2006**, *128*, 16073–16082.
- (54) Jimenez, R.; Fleming, G. R.; Kumar, P. V.; Maroncelli, M. Femtosecond Solvation Dynamics of Water. *Nature* **1994**, *369*, 471–473.
- (55) Stratt, R. M.; Cho, M. The Short-Time Dynamics of Solvation. *J. Chem. Phys.* **1994**, *100*, 6700–6708.
- (56) Rosenthal, S. J.; Xie, X.; Du, M.; Fleming, G. R. Femtosecond Solvation Dynamics in Acetonitrile: Observation of the Inertial Contribution to the Solvent Response. *J. Chem. Phys.* **1991**, *95*, 4715–4718.
- (57) Labastide, J. A.; Baghgar, M.; McKenna, A.; Barnes, M. D. Time- and Polarization-Resolved Photoluminescence Decay from Isolated Polythiophene (P3HT) Nanofibers. *J. Phys. Chem. C* **2012**, *116*, 23803–23811.
- (58) Andersson, P. O.; Gillbro, T. Photo-physics and Dynamics of the Lowest Excited Singlet State in Long Substituted Polyenes with Implications to the Very Long-Chain Limit. *J. Chem. Phys.* **1995**, *103*, 2509–2519.